



**University of
Zurich**^{UZH}

**Zurich Open Repository and
Archive**

University of Zurich
University Library
Strickhofstrasse 39
CH-8057 Zurich
www.zora.uzh.ch

Year: 2024

A novel estimator of Earth's curvature (allowing for inference as well)

Bell, David R ; Ledoit, Olivier ; Wolf, Michael

DOI: <https://doi.org/10.1214/23-aos1802>

Posted at the Zurich Open Repository and Archive, University of Zurich

ZORA URL: <https://doi.org/10.5167/uzh-260363>

Journal Article

Published Version

Originally published at:

Bell, David R; Ledoit, Olivier; Wolf, Michael (2024). A novel estimator of Earth's curvature (allowing for inference as well). *Annals of Applied Statistics*, 18(1):585-599.

DOI: <https://doi.org/10.1214/23-aos1802>

A NOVEL ESTIMATOR OF EARTH'S CURVATURE (ALLOWING FOR INFERENCE AS WELL)

BY DAVID R. BELL^{1,a}, OLIVIER LEDOIT^{2,b} AND MICHAEL WOLF^{2,c}

¹Idea Farm Ventures, ^adavid@ideafarmventures.com

²Department of Economics, University of Zurich, ^bolivier.ledoit@econ.uzh.ch, ^cmichael.wolf@econ.uzh.ch

This paper estimates the curvature of the Earth, defined as one over its radius, without relying on physical measurements. The orthodox model states that the Earth is (nearly) spherical with a curvature of $\pi/20,000$ km. By contrast, the heterodox flat-Earth model stipulates a curvature of zero. Abstracting from the well-worn arguments for and against both models, rebuttals and counter-rebuttals ad infinitum, we propose a novel statistical methodology based on verifiable flight times along regularly scheduled commercial airline routes; this methodology allows for both estimating and making inference for Earth's curvature. In particular, a formal hypothesis test resolutely rejects the flat-Earth model, whereas it does not reject the orthodox spherical-Earth model.

1. Introduction. This paper designs and executes an even-handed, replicable, and powerful test of the hypothesis that the Earth is flat against the hypothesis that the Earth is spherical. We accomplish this by developing an accurate estimator of the curvature of the Earth, defined as one over its radius, which allows for making inference as well. If the Earth is flat, its curvature is equal to zero; if it is instead spherical, according to the orthodox model, its curvature is equal to $\pi/20,000$ km = $1.5708 \cdot 10^{-4}$ km⁻¹.

This subject is of current policy interest because the flat-Earth movement is gathering strength, given its viral attractiveness in social networks. There are international societies, conferences, and widely distributed professional documentary films about it. Policy implications are especially heavy because the flat-Earth hypothesis flirts with the broader spectrum of conspiracy theories, such as: Was JFK assassinated by the FBI? Were the moon landings faked? Was 9/11 an inside job? Etc.

Testing for veracity or falsity is an arduous and socially valuable task because some conspiracy theories have historically turned out to be conspiracy facts. Just to give one big example: The entire Catholic Church hierarchy conspired to claim that the so-called “Donation of Constantine” had given them temporal control over Italy, and they got away with it for several centuries; however, it was fake news.

The flat-Earth hypothesis is also of scientific interest because the response from spherical-Earth proponents is usually limited to: (1) appeal to authority and (2) refusal to debate. Surely, astronauts or Antarctica explorers can opine and academics can publish papers that are not accessible to mere mortals, but this is not enough to satisfy the average educated, curious, and skeptical layperson.

As an example of appeal to academic authority, consider [Kuzii and Rovenchak \(2019\)](#). This paper is mathematically masterful but not readily accessible to those outside the narrow field of theoretical physics. Starting with Newton's law of gravitation, they derive expressions for the gravitational field of a two-dimensional mass, namely, the flat-Earth disk with radius R and constant surface density. In lay terms, the key qualitative insight is that the radial

component of gravitational force at distance r from the origin increases sharply and nonlinearly toward the “edge” of the disk, as the ratio r/R approaches one: An individual walking towards the edge of a flat Earth would, therefore, feel the need to bend as they walked or, alternatively, have the sensation that they were ascending up a “bowl” from the origin, as illustrated by [Kuzii and Rovenchak \(\(2019\), Figures 2 and 9\)](#), counter to actual sensorial experience.

Instead, such a fundamental question as whether the Earth is flat should ideally be decisively resolvable for free and without having to leave home or getting an advanced university degree. This is the epistemological gap the paper aims to fill.

We apply state-of-the-art statistical methodology in an innovative design to reverse-engineer three-dimensional information about Earth’s curvature from data collected on the two-dimensional manifold that is the surface of the Earth. The only data needed are: (i) longitude, (ii) distance from the North Pole, and (iii) flight times between airports connected by regularly scheduled commercial routes. Both flat-Earth and spherical-Earth models agree on the first two items. The third item is essentially unfalsifiable due to the large number of sources that report aviation data, so it will act as the “Judge of Peace” in the statistical analysis.

First, we establish an accurate relation between (average) flight time and distance using the routes where the two models most agree: along a north-south axis (allowing for North Pole flyover). We obtain an estimated linear model with an adjusted R^2 of 99.9% that must be acceptable to both camps. Second, we use this relation to execute a powerful test using the routes where the two models most *disagree*: along an east-west axis far away from the North Pole. This even-handed test resolutely rejects the flat-Earth model, whereas it does not reject the orthodox spherical-Earth model.

The crucial breakthrough is to reverse-engineer from surface data an estimator of the curvature of the Earth (and by implication its radius) that enjoys a near-perfect 99.3% relative accuracy just by applying the statistical method on publicly available and verifiable data without relying on complex (and expensive) physical measurements.

The remainder of the paper is organized as follows. Section 2 develops a general formula for the distance between two points on Earth that embeds both the flat-Earth and spherical-Earth models as special cases of a “curvature” parameter. Section 3 establishes an accurate relation between (average) flight time and distance using airline routes along a north-south axis (allowing for North Pole flyover), where the two models are in agreement with respect to distance between airports. Section 4 uses this relation to execute a formal hypothesis test by focusing on airline routes where the flat-Earth model and spherical-Earth model are most in disagreement: the ones along an east-west axis far from the North Pole. Section 5 concludes by reaffirming the core insights of our paper, namely, that it is possible to accurately reverse-engineer three-dimensional information about Earth’s curvature using only surface data as well as to decisively and irrefutably settle the lingering dispute between the flat-Earth and spherical-Earth proponents by designing and executing a test that is not only even-handed and replicable but also rests on elemental trigonometry only and is couched in terms of data that are intuitive and verifiable to a layperson. The Supplementary Material [Bell, Ledoit and Wolf \(2024\)](#) contains mathematical proofs and additional material.

2. Integrated model of distance between two points. This is a tale of two maps. It takes a model to beat a model: If flat-Earthers did not have a map to call their own, running any test would be like trying to nail jelly to a wall.

2.1. *The map of the flat Earth.* Thankfully, there exists a map that is well-accepted within the flat-Earth community. It is the polar azimuthal equidistant projection of the orthodox

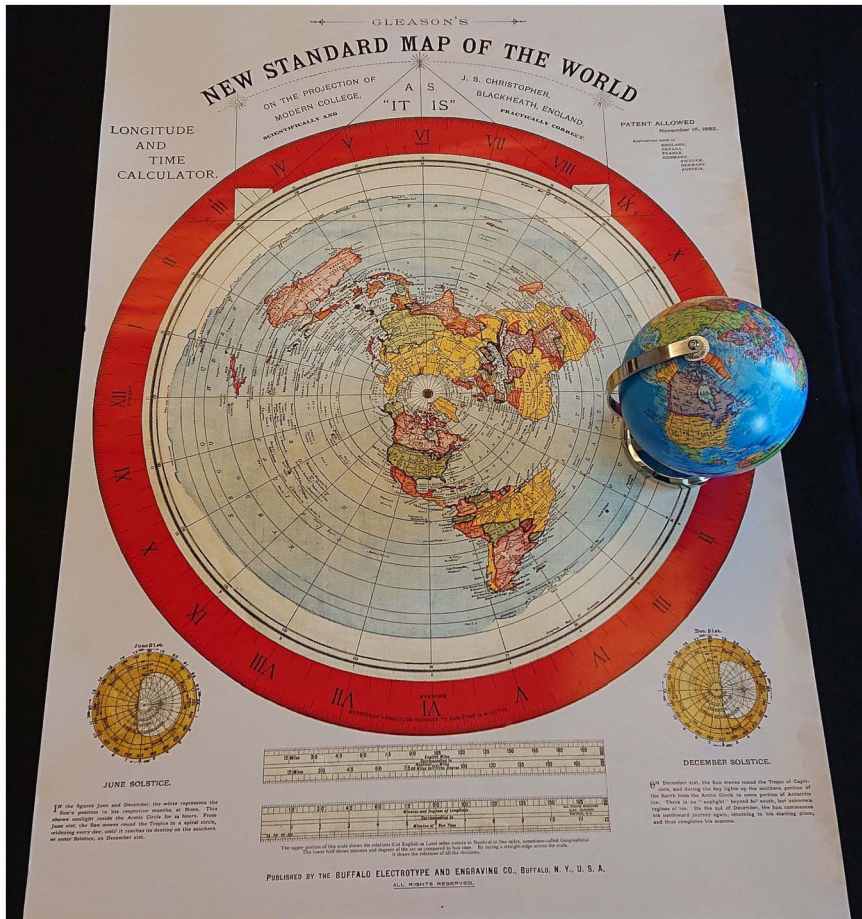


FIG. 1. Flat-Earth map and spherical-Earth globe on the same scale.

globe, centered on the North Pole. This well-known geometric construct (Snyder (1987), p. 192) means that flat-Earthers and spherical-Earthers agree on two measurements: (i) longitude and (ii) distance from the North Pole of a given city. As an illustration, Figure 1 displays side-by-side the heterodox flat-Earth map and the orthodox spherical-Earth globe.¹

The organizers of the 2018 Flat Earth International Conference had Alexander Gleason's flat-Earth map marketed during their event, as evidenced by the documentary *Flat Earth: To the Edge and Back* (at the 21- and 24-minute marks).² In addition, it conforms one-to-one with two other prestigious maps in the flat-Earth community: the one drawn by the movement's founder (Rowbotham (1881), Figure 54) and the one promoted on the current Flat Earth Society's website. It also coincides with two more maps of strong historical and political significance; see Bell, Ledoit and Wolf (2024), Appendix B.

On this basis, we can safely conclude that flat-Earth proponents coalesce around Gleason's 1892 north-polar azimuthal equidistant projection as a fair and legitimate representation of their belief system.

At the epistemological level, the flat-Earth Gleason map and the spherical-Earth orthodox globe are falsifiable. It means that both of them are not religions but *scientific* theories,

¹Although the globe is a three-dimensional object, it can also be called a "map" because it is a diagrammatic representation that shows the relative positions of identifiable points.

²The serious flat-Earth activist Nathan Thompson also promoted the same map in his segment of the high-profile 2018 Netflix documentary *Beyond the Curve*, starting at the 14-minute mark.

according to Popper (1959), and as such earn the right to an even-handed treatment. Nonetheless, they are so incompatible with each other, as illustrated by Figure 1, that designing an easily replicable, yet powerfully conclusive statistical analysis that falsifies either one or the other lies well within the reach of determined statisticians.

2.2. Longitude. Longitude is an angular measure centered on the North Pole computed relative to a reference meridian. The reference (or “prime”) meridian is traditionally taken as the one that radiates out of the North Pole through the Greenwich Royal Observatory (just across the River Thames from London) and beyond. The flat-Earth map of Figure 1 indicates (in small print) the Greenwich meridian extending to the right of the North Pole. A city’s longitude is customarily expressed as a number of degrees in the $[0^\circ, 180^\circ]$ range, either east or west of Greenwich. Not all meridians can be shown on a map, of course; the flat-Earth map in Figure 1 shows all meridians that are integer multiples of 15° . For the purpose of the upcoming test, it is practical to deviate from custom and convert longitude from degrees into radians (which we denote by θ) as follows.

DEFINITION 2.1.

1. If a point has longitude conventionally expressed in degrees as $d^\circ m' s''$ east, then its longitude expressed in radians is

$$(2.1) \quad \theta := \frac{\pi}{180^\circ} \left(d + \frac{m}{60} + \frac{s}{60^2} \right).$$

2. If a point has longitude conventionally expressed in degrees as $d^\circ m' s''$ west, then its longitude expressed in radians is

$$(2.2) \quad \theta := -\frac{\pi}{180^\circ} \left(d + \frac{m}{60} + \frac{s}{60^2} \right).$$

This mapping of longitudes into radians $\theta \in [-\pi, \pi]$ is valid in both the flat-Earth model and the spherical-Earth model. The sign comes from the trigonometric convention that turning counterclockwise is positive.

2.3. Distance from the North Pole. Distance from the North Pole, according to the flat-Earth map in Figure 1, can be inferred from the legend at the bottom that says “60 nautical miles to the degree.” Given that the North Pole is at 90 degrees of latitude relative to the Equator, this implies that the distance from the North Pole to the Equator is $60 \times 90 = 5400$ nautical miles. A helpful double-sided ruler also shows that there are 208 land miles (what we would now call U.S. miles) to 180 nautical miles; however, the more accurate ratio is 207.6 U.S. miles to 180.4 nautical miles. It implies that the distance from the North Pole to the Equator is $5400 \times 207.6/180.4 = 6214$ U.S. miles. Given that there are 1.6093 U.S. miles to the kilometer, we finally get a distance from the North Pole to the Equator of $6214 \times 1.6093 = 10,000$ km. This is the same distance as in the spherical-Earth model because the meter was precisely defined by the French Revolution as the $(1/10,000,000)$ th part of the distance from the North Pole to the Equator.

There is no surprise here: Polar azimuthal projection preserves distance from the North Pole, but it was worth double-checking by hand. The correspondence runs much deeper though, as any two cities on the same meridian have the same distance (both in terms of centimeters on the map and corresponding kilometers in the real world) on the flat-Earth map and the spherical-Earth globe; the scale is 11 centimeters to 10,000 kilometers. This is even true when two cities are on anti-meridians (meaning 180° apart from each other) if they are both north of the Equator.

This is the how we can say that the two maps in Figure 1 are on the same scale. Visual confirmation comes easily because Canada has basically the same shape and size in both the flat-Earth map and the orthodox globe. Once again, the requirements of our test make us depart from convention by using not latitude (expressed in degrees north or south away from the Equator) but instead distance from the North Pole.

PROPOSITION 2.2. Define the constant $c^S := \frac{\pi}{20,000 \text{ km}}$:

1. If a point has latitude $d^\circ m' s''$ north, then its distance from the North Pole is

$$(2.3) \quad r = \frac{\pi}{180^\circ} \left[90^\circ - \left(d + \frac{m}{60} + \frac{s}{60^2} \right) \right] \times \frac{1}{c^S}.$$

2. If a point has latitude $d^\circ m' s''$ south, then its distance from the North Pole is

$$(2.4) \quad r = \frac{\pi}{180^\circ} \left[90^\circ + \left(d + \frac{m}{60} + \frac{s}{60^2} \right) \right] \times \frac{1}{c^S}.$$

These two statements are valid in both the flat-Earth model and the spherical-Earth model.

The constant $c^S := \pi/20,000 \text{ km}$ is equal to one over the radius of the Earth if the Earth is spherical according to the orthodox model,³ so it represents the *curvature* of the Earth (or, one could also say, of the meridians) in the orthodox model. If the Earth is flat, c^S does not serve to measure curvature anymore, but it still serves to convert latitude into distance from the North Pole.

The first reason why we insist on defining the location of a specific point on the Earth by using the pair (r, θ) is that both the flat-Earth model and the spherical-Earth model agree on (r, θ) . The second reason is that (r, θ) constitute what is known as a pair of *polar coordinates*, which facilitates usage of standard trigonometric techniques.

2.4. *Distance between two points in the flat-Earth model.* We can now give the formula for the distance between any two points on the flat Earth.

THEOREM 2.3. Consider two points with polar coordinates (r_1, θ_1) and (r_2, θ_2) , respectively. In the flat-Earth model, the distance between these two points is equal to

$$(2.5) \quad d^F(r_1, \theta_1; r_2, \theta_2) = \sqrt{r_1^2 + r_2^2 - 2r_1r_2 \cos(\theta_1 - \theta_2)}.$$

This is what one would find by using a hand-held ruler to measure the length of a straight line between any two cities on the flat-Earth map in Figure 1.

2.5. *Distance between two points in the spherical-Earth model.* To continue the parallel examination of the orthodox spherical-Earth model alongside its heterodox flat-Earth rival, we now present a counterpart to Theorem 2.3.

THEOREM 2.4. Consider two points with polar coordinates (r_1, θ_1) and (r_2, θ_2) , respectively. In the spherical-Earth model, the distance $d^S(r_1, \theta_1; r_2, \theta_2)$ between these two points is equal to

$$(2.6) \quad \frac{1}{c^S} \arccos \left\{ \cos^2 \left(\frac{\theta_1 - \theta_2}{2} \right) \cos[(r_1 - r_2)c^S] + \sin^2 \left(\frac{\theta_1 - \theta_2}{2} \right) \cos[(r_1 + r_2)c^S] \right\}.$$

³Hence, the superscript S in c^S .

This formula is particularly intuitive in two cases:

1. If both points are on the same meridian, then $\cos^2(\frac{\theta_1-\theta_2}{2}) = 1$ and $\sin^2(\frac{\theta_1-\theta_2}{2}) = 0$, so the output is the difference between the two distances from the North Pole. This corresponds to a path that does not go through a pole.
2. If the two points are on antimeridians relative to each other, then $\cos^2(\frac{\theta_1-\theta_2}{2}) = 0$ and $\sin^2(\frac{\theta_1-\theta_2}{2}) = 1$, so the output depends on the sum of the two distances from the North Pole. This corresponds to a path that goes through a pole.

In the general case, since $\cos^2(\frac{\theta_1-\theta_2}{2}) + \sin^2(\frac{\theta_1-\theta_2}{2}) = 1$, the distance will be a weighted average of the distance implied by the difference $r_1 - r_2$ (not going through/near a pole) and the one implied by the sum $r_1 + r_2$ (going through/near a pole), with their relative importances controlled by the difference of longitudes $\theta_1 - \theta_2$. Once again, this is what we would find if we used a flexible measuring tape on the orthodox globe in Figure 1.

2.6. *Making curvature a free input.* This section contains our final mathematical result: an integrated formula for distance that embeds both the spherical-Earth model and the flat-Earth model as special cases, depending on how the curvature parameter is dialed up or down.

THEOREM 2.5. *Define the distance function $D(r_1, \theta_1; r_2, \theta_2; c)$ as*

$$(2.7) \quad \begin{cases} \frac{1}{c} \arccos \left\{ \cos^2 \left(\frac{\theta_1 - \theta_2}{2} \right) \cos[(r_1 - r_2)c] \right. \\ \left. + \sin^2 \left(\frac{\theta_1 - \theta_2}{2} \right) \cos[(r_1 + r_2)c] \right\} & \text{if } c > 0, \\ \sqrt{r_1^2 + r_2^2 - 2r_1r_2 \cos(\theta_1 - \theta_2)} & \text{if } c = 0, \end{cases}$$

on the domain $\{(r_1, \theta_1; r_2, \theta_2; c) \in \mathbb{R}^4 : r_1 \geq 0, r_2 \geq 0, c \geq 0, r_1c \leq \pi, r_2c \leq \pi\}$.

The function D is continuous on its domain of definition.

The function D embeds both the spherical-Earth distance function as the special case $c = c^S$ and the flat-Earth distance function as the special case $c = 0$. Having c as a free input (parameter) will allow us to construct an estimator of Earth’s curvature as well as a test of the flat-Earth model against the spherical-Earth model. In order to implement such statistical methodology in practice, Section 3 will need to establish an accurate relation between (average) flight time and distance that is easy to verify from publicly available data.

At the epistemological level, moving from the spherical-Earth model to the flat-Earth model (or vice-versa, as has been the case in the distant past) would constitute a paradigm shift in the sense of Kuhn (1962). The structure of scientific revolutions is such that they are either-or propositions: you are either with the old paradigm or with the new one, and there is nothing in-between. This makes cogent evaluation of the relative merits of both camps extremely contentious. The value of Theorem 2.5 is that it integrates both paradigms into a broader continuum that restores the possibility of civilized testability.

3. Relation between flight time and distance. In order to establish an accurate relation between (average) flight time of regularly scheduled commercial aircraft and the distance between two points on the surface of the Earth, in a way that is acceptable to all, our initial focus will be on airline routes where the flat-Earth model and the spherical-Earth model most agree.

3.1. *Geometric analysis of agreement.* Pairs of locations for which both models give the same distance are identified by the following theorem.

THEOREM 3.1. *Consider two points with polar coordinates (r_1, θ_1) and (r_2, θ_2) , respectively. Then $d^F(r_1, \theta_1; r_2, \theta_2) = d^S(r_1, \theta_1; r_2, \theta_2)$ if either one of the two following conditions is satisfied:*

Condition 1: *The points are on the same meridian ($\theta_1 = \theta_2$).*

Condition 2: *The points are on antimeridians ($|\theta_1 - \theta_2| = \pi$) and $r_1 + r_2 \leq 20,000$ km.*

3.2. *Airport pairs on a north-south axis.* Manual exploration of the site flightsfrom.com yields 10 commercial airline routes (listed in Table 1) that almost perfectly (a.p.) satisfy the conditions of Theorem 3.1. The first eight routes (a.p.) satisfy Condition 1 (same meridian) and the last two routes (a.p.) satisfy Condition 2 (antimeridian, flying through the North Pole route). The distances between airports have been obtained from the original latitude and longitude data by following the derivations of Section 2. Just to illustrate and for the sake of clarity, we can provide a fully worked-out example of the calculations for the distances between Johannesburg and Istanbul in the first row of Table 1. Applying Proposition 2.2 and Definition 2.1, respectively, to the latitude and longitude data yields

$$\begin{aligned} \text{Johannesburg:} \quad r_1 &= 12,904 \text{ km} & \theta_1 &= 0.4931 \text{ rad} \\ \text{Istanbul:} \quad r_2 &= 5415 \text{ km} & \theta_2 &= 0.5014 \text{ rad} \end{aligned}$$

Based on these four inputs, both formulas (2.5) and (2.6) give a distance of 7489 km (rounding to the nearest integer). Readers are encouraged to double-check these computations independently, as they are technically central to the paper.

TABLE 1
Ten airport pairs with essentially identical flat-Earth and spherical-Earth distances

City	Airport	Latitude	Longitude	r (km)	θ (rad)	d^F (km)	d^S (km)
Johannesburg (RSA)	JNB	26°08'00"S	28°15'00"E	12,904	0.4931	7489	7489
Istanbul (Turkey)	IST	41°15'44"N	28°43'40"E	5415	0.5014		
Santiago (Chile)	SCL	33°23'34"S	70°47'08"W	13,710	-1.2354	8238	8232
New York (USA)	JFK	40°38'23"N	73°46'44"W	5484	-1.2877		
Frankfurt (Germany)	FRA	50°02'00"N	08°34'14"E	4441	0.1496	4561	4560
Abuja (Nigeria)	ABV	09°00'24"N	07°15'47"E	8999	0.1268		
Abu Dhabi (UAE)	AUH	24°25'59"N	54°39'04"E	7285	0.9538	3237	3236
Mahé (Seychelles)	SEZ	04°40'28"S	55°31'19"E	10,519	0.9690		
London (UK)	LHR	51°28'39"N	00°27'41"W	4280	-0.0081	5097	5097
Accra (Ghana)	ACC	05°36'17"N	00°10'03"W	9377	-0.0029		
Melbourne (AUS)	MEL	37°40'24"S	144°50'36"E	14,186	2.5280	8191	8173
Tokyo (Japan)	NRT	35°45'55"N	140°23'08"E	6026	2.4502		
Hong Kong (China)	HKG	22°18'32"N	113°54'52"E	7521	1.9882	6039	6032
Perth (AUS)	PER	31°56'25"S	115°58'01"E	13,549	2.0240		
Cape Town (RSA)	CPT	33°58'10"S	18°35'50"E	13,774	0.3246	9433	9386
Frankfurt (Germany)	FRA	50°02'00"N	08°34'14"E	4441	0.1496		
Dubai (UAE)	DXB	25°15'10"N	55°21'52"E	7194	0.9663	13,403	13,390
Los Angeles (USA)	LAX	33°56'33"N	118°24'29"W	6229	-2.0666		
Doha (Qatar)	DOH	25°16'23"N	51°29'36"E	7192	0.8987	12,994	12,983
San Francisco (USA)	SFO	37°37'08"N	122°22'30"W	5820	-2.1358		

TABLE 2

Average flight times between 10 airport pairs with essentially identical flat-Earth and spherical-Earth distances

Airline	Route	Flight #	Flight time	Average
Turkish Airlines	Johannesburg → Istanbul	TK41	08 h 42 min	08 h 44 min
	Istanbul → Johannesburg	TK40	08 h 46 min	
LATAM Airlines	Santiago → New York	LA532	09 h 50 min	09 h 41 min
	New York → Santiago	LA533	09 h 33 min	
Lufthansa	Frankfurt → Abuja	LH594	05 h 37 min	05 h 39 min
	Abuja → Frankfurt	LH595	05 h 40 min	
Etihad Airways	Abu Dhabi → Mahé	EY622	04 h 17 min	04 h 13 min
	Mahé → Abu Dhabi	EY621	04 h 10 min	
British Airways	London → Accra	BA81	06 h 06 min	06 h 12 min
	Accra → London	BA78	06 h 18 min	
Japan Airlines	Melbourne → Tokyo	JL774	09 h 21 min	09 h 27 min
	Tokyo → Melbourne	JL773	09 h 33 min	
Cathay Pacific	Hong Kong → Perth	CX171	07 h 01 min	07 h 04 min
	Perth → Hong Kong	CX170	07 h 07 min	
Lufthansa	Cape Town → Frankfurt	LH577	11 h 18 min	11 h 13 min
	Frankfurt → Cape Town	LH576	11 h 07 min	
Emirates Airlines	Dubai → Los Angeles	EK215	15 h 33 min	15 h 23 min
	Los Angeles → Dubai	EK216	15 h 13 min	
Qatar Airways	Doha → San Francisco	QR737	15 h 02 min	14 h 52 min
	San Francisco → Doha	QR738	14 h 42 min	

Disagreement between the two models is exceedingly small for all of the 10 airport pairs listed in Table 1: It ranges from zero to only 47 kilometers at most, never exceeding 1% of the flight distance.

3.3. *Flight times along a north-south axis.* We collect flight times over the routes in Table 1 from [flightaware.com](https://www.flightaware.com). These are defined as the average take-off-to-landing time over all the flights that took place over a three-month window.⁴ The data were manually collected from the website on 12 November 2022, and go as far back as 12 August 2022. We carried out an independent check over the 10 most recent flights with a competitor site, [airportia.com](https://www.airportia.com), and found negligible discrepancies of only a few minutes at most. Gate-to-gate times are slightly longer because of taxiing around the runway; [flightaware.com](https://www.flightaware.com) reports those too, and they match on average what the airline itself has announced, which is yet another independent check.

Given the economic incentives for airlines, the needs of passengers, and their ability to transmit and propagate information about flight arrival and departures via social networks as well as oversight by regulatory authorities, it is simply not possible to cheat on such data systematically, let alone by a wide margin.

REMARK (Average flight time). Each “flight time” in column four of Table 2, and later in Table 4, is actually an average of many individual flight times collected; but in order to keep terminology compact, what we mean by “average flight time” listed in column 5 of the two tables is the average of the two “flight times” in column 4 (to and fro). Clearly, we need

⁴The number of flight times over which we average depends on the sample size for any given route in Table 2; the mean and median of the 20 sample sizes are, roughly, equal to 65.

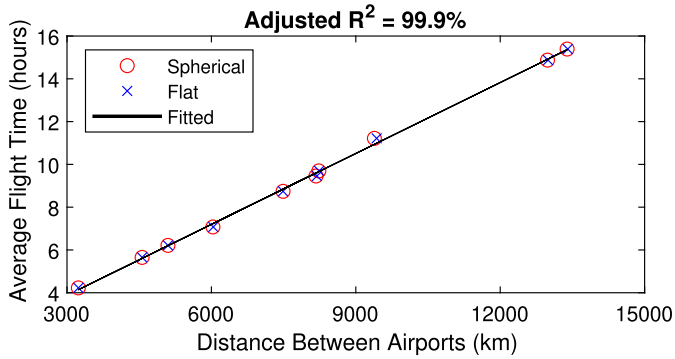


FIG. 2. Linear regression of average flight time on a constant and distance along a north-south axis.

to work with this overall average flight time in order to eliminate (or at least mitigate) effects of head and tail winds.

3.4. *Regressing average flight time on distance.* Having gathered airport-pair-distance data (Table 1) and flight-time data along the same routes (Table 2), we are now ready to fit a linear regression model of average flight time on distance for a generic flight. Given the visible and obvious agreement between the flat-distance column and the spherical-distance column in Table 1, this model should be equally agreeable to flat-Earthers and spherical-Earthers alike. The model specification is grounded in the fundamental premise that engineering and economic constraints governing the modern airline industry dictate that average flight times depend on distance and little else.

As widely reported in the popular and business press, average flight times have, counterintuitively, increased despite advances in technology; for example, see Ledsom (2022). These increases are attributed to practices like “schedule padding” and the desire to save money on fuel; recall, however, that our data collection window was a mere three months, obviating any issues in our case.

We stack the vector of 10 spherical-Earth distances atop the vector of 10 flat-Earth distances to construct an independent variable (or regressor) of dimension 20×1 , which we call X . We then stack two copies of the corresponding average flight times on top of each other to construct a dependent variable (or regressand) of dimension 20×1 , which we call Y . Finally, we regress Y (unit: hours) on a constant and X (unit: kilometers) via ordinary least squares. The result is

$$(3.1) \quad \hat{Y} = \frac{34}{60} \text{ h} + \frac{X}{905 \text{ km/h}}.$$

This means that in order to predict average flight times, we just need to charge a constant penalty of 34 minutes for the initial climb after takeoff and the final descent before landing and assume an average cruising speed of 905 km/h that carries the aircraft from departure point to arrival point.

Figure 2 provides a graphical illustration. The adjusted R^2 of the estimated linear regression model (3.1) is a near-perfect 99.9%, so treating the relation as exact (over the range of observed distances in the data, or slightly outside of it) seems justified.

4. Testing the flat-Earth model. Whereas all the work so far has been to establish commonalities between the flat-Earth model and the spherical-Earth model in order to establish an (essentially) exact relation between (average) flight time and distance, we now turn to the *maximal disagreement* in order to set up a powerful test of the flat-Earth model.

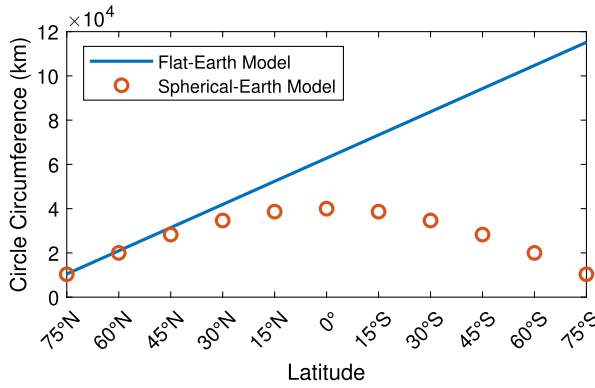


FIG. 3. Implied circumferences of the 11 major parallel circles.

4.1. *Geometric analysis of disagreement: Latitude & parallels.* The main difference between the two models is quite obvious: It lies in the implied circumferences of the 11 parallel circles visible in Figure 1. A parallel circle is the ensemble of all the points on the surface of the Earth that are at the same distance from the North Pole.

In extracting information from Gleason’s map, we ignore the Arctic and Antarctic Circles (both clearly labeled) as well as the Tropics of Capricorn and Cancer (one labeled, the other one not but still clearly identifiable). These four traditional circles pertain more to the solar cycle of seasons than to the geometry of the surface of the Earth itself. The pertinent information lies in the 11 circles that are labeled from 0° to 75° in 15° latitude intervals on both sides of the Equator. Regarding the contentious 90° south parallel circle, which may or may not reduce to a single point, we can safely omit it since no regular commercial airline route flies over Antarctica.

Because of the geometry of the polar azimuthal equidistant projection, parallel circles go through the same cities in the flat-Earth model as in the spherical-Earth model. Not all parallel circles can be represented on a map, of course, so it is only the major ones, the ones on 15° latitude intervals, that are plotted. Figure 3 shows how the perimeters of the major parallel circles according to the two respective models diverge as one moves further away from the North Pole.

The two formulas used to generate Figure 3 are, for latitude $\ell \in \{0^\circ, 15^\circ, \dots, 75^\circ\}$,

$$(4.1) \quad C^F(\ell) := \begin{cases} 2\pi \frac{90^\circ - \ell}{90^\circ} \times 10,000 \text{ km} & \text{if north,} \\ 2\pi \times 10,000 \text{ km} & \text{if } \ell = 0^\circ, \\ 2\pi \frac{90^\circ + \ell}{90^\circ} \times 10,000 \text{ km} & \text{if south,} \end{cases}$$

$$(4.2) \quad C^S(\ell) := 4 \cos\left(\pi \frac{\ell}{180^\circ}\right) \times 10,000 \text{ km.}$$

REMARK (Deviations from perfect sphericity). Formula (4.2) for $C^S(\ell)$ assumes that the Earth is a perfect sphere in which case the circumference of the Equator is four times its distance from the North Pole. The mainstream view is more nuanced: The Earth is spherical only *approximately*; it is slightly flatter around the poles and bulges a little more around the Equator. In this paper we opt to ignore such refinements and instead treat the Earth as a perfect sphere for the sake of simplicity.

Figure 3 shows that initially, when one is close to the North Pole, in particular at 75° of latitude, there is very little difference between the circumferences implied by the two models.

TABLE 3
Ten airport pairs with strongly different flat-Earth and spherical-Earth distances

City	Airport	Latitude	Longitude	r (km)	θ (rad)	d^F (km)	d^S (km)
Santiago (Chile)	SCL	33°23'34''S	70°47'08''W	13,710	-1.2354	23,391	9646
Auckland (NZ)	AKL	37°00'29''S	174°47'30''E	14,112	3.0507		
Johannesburg (RSA)	JNB	26°08'00''S	28°15'00''W	12,904	0.4931	23,438	11,016
Sydney (AUS)	SYD	33°56'46''S	151°10'38''E	13,772	2.6385		
São Paulo (Brazil)	GRU	23°26'08''S	46°28'23''W	12,604	-0.8111	11,825	6529
Luanda (Angola)	LAD	08°51'30''S	13°13'52''E	10,984	0.2309		
Papeete (France)	PPT	17°33'24''S	149°36'41''W	11,951	-2.6112	9185	4629
Nouméa (France)	NOU	22°00'59''S	166°12'58''E	12,446	2.9010		
Auckland (NZ)	AKL	37°00'29''S	174°47'30''E	14,112	3.0507	13,593	5332
Perth (AUS)	PER	31°56'25''S	115°58'01E	13,549	2.0240		
Johannesburg (RSA)	JNB	26°08'00''S	28°15'00''W	12,904	0.4931	18,334	5882
Perth (AUS)	PER	31°56'25''S	115°58'01''E	13,549	2.0240		
Perth (AUS)	PER	31°56'25''S	115°58'01''E	13,549	2.0240	12,623	5882
Port Louis (Mauritius)	MRU	20°25'48''S	57°40'59''E	12,270	1.0068		
Easter Island (Chile)	IPC	27°09'53''S	109°25'18''E	13,018	-1.9098	8866	3749
Santiago (Chile)	SCL	33°23'34''S	70°47'08''W	13,710	-1.2354		
Wellington (NZ)	WLG	41°19'38''S	174°48'19''E	14,592	3.0509	7449	2588
Melbourne (AUS)	MEL	37°40'24''S	144°50'36''E	14,186	2.5280		
Singapore (Singapore)	SIN	01°21'33''N	103°59'22''E	9849	1.8150	14,174	8649
Johannesburg (RSA)	JNB	26°08'00''S	28°15'00''W	12,904	0.4931		

However, the difference gradually increases as one moves further away from the North Pole, and becomes huge beyond the Equator into the Southern Hemisphere. This feature allows us to construct a powerful test of the flat-Earth model against the spherical-Earth model.

4.2. *Airport pairs on an east-west axis far from the North Pole.* Using the three criteria highlighted below:

1. departure and arrival cities linked by a direct regularly scheduled commercial flight,
2. being as far away from the North Pole as possible,
3. and spanning an arc of longitude as wide as possible,

we put together in Table 3 a list of 10 airport pairs where the flat-Earth model and the spherical-Earth model strongly disagree with respect to distance. There is a wide variety of airports (14 in total), spanning Africa, South America, Oceania, and Asia. The average distance from the North Pole is 13,034 km, ranging from a minimum of 9849 km (Singapore) to a maximum of 14,592 km (Wellington). Longitudes (expressed in radians) are quite different between departure and arrival airports, meaning that the routes have a strong alignment with an east-west axis instead of a north-south axis.

4.3. *Flight times along an east-west axis.* As in Section 3.3, we collect the average takeoff-to-landing flight times between 12 August and 12 November 2022 from flightaware.com. These are reported in Table 4.⁵

⁵The number of flight times over which we average depends on the sample size for any given route in Table 4; both the mean and median of the 20 sample sizes are, roughly, equal to 50.

TABLE 4
Flight times for 10 airport pairs with strongly different flat-Earth and spherical-Earth distances

Airline	Route	Flight #	Flight time	Average
LATAM Airlines	Santiago → Auckland	LA801	12 h 04 min	11 h 08 min
	Auckland → Santiago	LA800	10 h 11 min	
Qantas Airways	Johannesburg → Sydney	QF64	11 h 16 min	12 h 28 min
	Sydney → Johannesburg	QF63	13 h 40 min	
Angola Airlines	São Paulo → Luanda	DT748	07 h 58 min	08 h 08 min
	Luanda → São Paulo	DT747	08 h 17 min	
Aircalin	Papeete → Nouméa	SB601	06 h 06 min	05 h 36 min
	Nouméa → Papeete	SB600	05 h 06 min	
Air New Zealand	Auckland → Perth	NZ175	06 h 41 min	06 h 11 min
	Perth → Auckland	NZ176	05 h 40 min	
Qantas Airways	Johannesburg → Perth	QF66	08 h 57 min	09 h 49 min
	Perth → Johannesburg	QF65	10 h 40 min	
Air Mauritius	Perth → Port Louis	MK441	07 h 50 min	07 h 03 min
	Port Louis → Perth	MK440	06 h 17 min	
LATAM Airlines	Easter Island → Santiago	LA842	04 h 13 min	04 h 29 min
	Santiago → Easter Island	LA841	04 h 44 min	
Qantas Airways	Wellington → Melbourne	QF172	03 h 34 min	03 h 21 min
	Melbourne → Wellington	QF171	03 h 09 min	
Singapore Airlines	Singapore → Johannesburg	SQ478	09 h 58 min	09 h 58 min
	Johannesburg → Singapore	SQ479	09 h 59 min	

4.4. *Statistical analysis.* We have now gathered all the building blocks to construct an estimator of Earth's curvature, along with corresponding inference. In order to conduct the analysis, we map distances into average flight times using model (3.1),

$$(4.3) \quad T(r_{i,1}, \theta_{i,1}; r_{i,2}, \theta_{i,2}; c) := \frac{34}{60} \text{ h} + \frac{D(r_{i,1}, \theta_{i,1}; r_{i,2}, \theta_{i,2}; c)}{905 \text{ km/h}},$$

where $(r_{i,1}, \theta_{i,1})$ are the polar coordinates of the first-listed airport on route $i = 1, \dots, 10$, as recorded in Table 3, $(r_{i,2}, \theta_{i,2})$ are the polar coordinates of the second-listed one, D is the integrated formula for distance from Theorem 2.5, and c is the (unknown) true curvature. The curvature c is then estimated via nonlinear least squares,

$$\hat{c} := \operatorname{argmin}_{\tilde{c}} \sum_{i=1}^{10} [Y_i - T(r_{i,1}, \theta_{i,1}; r_{i,2}, \theta_{i,2}; \tilde{c})]^2,$$

where Y_i is the average flight time for route i , as recorded in the last column of Table 4, and the “candidate” value \tilde{c} can range over the domain $[0, \min(\min_i(\pi/r_{i,1}), \min_i(\pi/r_{i,2}))]$. The results⁶ are as follows:

$$\hat{c} = 1.5779 \cdot 10^{-4} \quad \text{and} \quad \text{SE}(\hat{c}) = 4.9813 \cdot 10^{-7},$$

where the standard error $\text{SE}(\hat{c})$ is computed according to Greene (2008, Theorem 11.2); note that we use the degree-of-freedom correction for $\hat{\sigma}^2$ with $K = 1$ outlined below (Greene (2008), equation (11-13)).

⁶For the sake of exposition, we omit the unit (km) from all radius and curvature values in this section.

A classic (or normal-theory) nominal 95% confidence interval for c is then given by

$$(4.4) \quad \hat{c} \pm 1.96 \cdot \text{SE}(\hat{c}) = [1.5681 \cdot 10^{-4}, 1.5876 \cdot 10^{-4}].$$

Alternatively, with the aim of more reliable small-sample inference, one can use the studentized symmetric bootstrap based on resampling cases; for example, see [Davison and Hinkley \(1997\)](#), Sections 6.2 and 7.4. In this way one obtains a nominal 95% bootstrap confidence interval as

$$(4.5) \quad \hat{c} \pm t_{0.95}^{|\cdot|,*} \cdot \text{SE}(\hat{c}) = [1.5674 \cdot 10^{-4}, 1.5883 \cdot 10^{-4}].$$

Here $t_{\lambda}^{|\cdot|,*}$ denotes the bootstrap estimate of the λ quantile of the sampling distribution of

$$\frac{|\hat{c} - c|}{\text{SE}(\hat{c})},$$

which we base on $R = 99,999$ bootstrap repetitions. As is often the case with small sample sizes, the bootstrap confidence interval is somewhat wider than the classic confidence interval, the reason being that

$$t_{0.95}^{|\cdot|,*} = 2.094 > 1.96.$$

Nevertheless, both intervals come to the same conclusion: Whereas the flat-Earth model is rejected, the spherical-Earth model is not. This is because whereas both intervals do not contain zero, they do contain $c^S := \pi/20,000 = 1.5708 \cdot 10^{-4}$.

Another way to carry out inference on the flat-Earth model is to compute a p -value for the one-sided hypothesis testing problem

$$H_0 : c = 0 \quad \text{vs.} \quad H_1 : c > 0.$$

The test statistic computed from the observed data is given by

$$t := \frac{\hat{c}}{\text{SE}(\hat{c})} = \frac{1.5779 \cdot 10^{-4}}{4.9813 \cdot 10^{-7}} = 316.8.$$

Therefore, the classic p -value is given by

$$p = \text{Prob}(X \geq 316.8) \quad \text{with } X \sim N(0, 1),$$

where $N(0, 1)$ denotes the standard normal distribution. This results in $p = 0$ using statistical software (up to machine precision). Alternatively, following the convention in [Davison and Hinkley \(\(1997\), Section 4.4\)](#), the bootstrap p -value is given by

$$p = \frac{1 + \#\{t_r^* \geq t\}}{R + 1} \quad \text{with } t_r^* := \frac{\hat{c}_r^* - \hat{c}}{\text{SE}(\hat{c}_r^*)},$$

where we still use resampling cases (without enforcing the null hypothesis in the bootstrap distribution). This results in $p = 1/(R + 1)$ for any number of bootstrap repetitions R we tried. For example, the number $R = 99,999$ results in a bootstrap p -value of $p = 0.00001$. Obviously, an even smaller p -value can be obtained by increasing the number R , but doing so makes no practical difference.

Last but not least, by inverting the endpoints of the confidence intervals (4.4)–(4.5) for Earth's curvature c one can back out nominal 95% classic and bootstrap confidence intervals for Earth's radius $1/c$ as

$$(4.6) \quad [6299, 6377], \quad \text{respectively,} \quad [6296, 6380].$$

Obviously, both intervals contain the the orthodox value $1/c^S = 20,000/\pi = 6366$.

Since the point estimate of Earth's radius is given by $1/\hat{c} = 1/1.5779 \cdot 10^{-4} = 6338$, even the somewhat wider bootstrap confidence interval implies a relative accuracy of 99.3%, where we define *relative accuracy* as one minus the ratio of margin of error to point estimate. For symmetric confidence intervals, which (up to the provided precision) both intervals in (4.6) are, the margin of error is given by half the width of the interval, that is, by the distance from the point estimate to either end point of the interval. Therefore, we obtain the following relative accuracy based on the bootstrap confidence interval: $1 - (6380 - 6338)/6338 = 0.9933$.

4.5. *Discussion.* The results of our statistical analysis have been obtained by making some simplifying assumptions:

1. In the spherical-Earth model, the Earth is perfectly spherical.
2. The mapping from distances to average flight times, estimated via linear regression on north-south routes, was used as if it held perfectly.
3. The small sample ($n = 10$) that we have collected synthesizes the information content of the other regularly-scheduled commercial airline routes not downloaded.

Having said that, none of these limitations, even taken together, really matter in the end: Even if we increased the widths of the confidence intervals (4.4)–(4.5) by a factor of 10, the flat-Earth model would still be rejected.

Our contribution to a topic uniquely intriguing in both scientific discourse and in popular culture is that we managed to conclusively discriminate between two strongly opposing physics models without doing any physics experiment or physics theory. Rather, we have simply and carefully applied the statistical method. It is usually hard to change one's mind (let alone someone else's mind) about a belief held; but for the proponents of the flat-Earth model, we suggest an easy way to do so: Take one of the flights listed in Table 4 and time it with your own watch. (Strictly speaking, take a round-trip flight and then record the average flight time.)

Sometimes a simple picture that distills the essence of the result is a good way to summarize the main point. There are two flights from Perth (Western Australia) that take almost exactly seven hours on average: due north to Hong Kong, and due west to Mauritius. Given near-identical average flight durations, the distances should match too. They do not if the Earth is flat, but they do if it is spherical, as Figure 4 illustrates.

If the Earth were flat, Perth–Mauritius should take twice as long as Perth–Hong Kong, which it does not. The fundamental contradiction is that, under the flat-Earth model, flight durations observed on an east-west axis far away from the North Pole are incompatible with flight durations observed on a north-south axis.

5. Conclusion. We have carried out a side-by-side evaluation of the heterodox flat-Earth model against the orthodox spherical-Earth model, without a priori favoring one over the other. The key was to use, as an instrument, the distance between airport pairs connected by regularly scheduled commercial flights, whose times of departure and arrival are essentially unfalsifiable public knowledge.

We first selected airport pairs for which both models give (essentially) the same distance, namely, airport pairs on a north-south axis that are either on the same meridian or on an antimeridian with a combined distance from the North Pole less than or equal to 20,000 km. We used these selected routes to establish an accurate relation between (average) flight time and distance that should be acceptable to advocates of both models and then selected flight routes along an east-west axis far away from the North Pole to set up a powerfully discriminant test between the two.



FIG. 4. Perth–Hong Kong and Perth–Mauritius lines drawn in black.

The outcome is that observed flight durations along an east-west axis far from the North Pole are too short to be compatible with those along a north-south axis if the Earth is flat. This test decisively rejects the flat-Earth model in favor of the spherical-Earth model. Our novel test's main and compelling advantages are: (i) its simple yet powerful design, (ii) its use of easily verifiable and uncontroversial data, and (iii) the fact that it was executed in an even-handed and disinterested way. What is more, we have demonstrated that the statistical method can estimate a physics quantity as important as Earth's curvature with a remarkably high relative accuracy of 99.3%, without relying on any physical measurements whatsoever.

Acknowledgments. The authors would like to thank an Associate Editor and the Editor for their constructive comments that improved the quality of this paper.

SUPPLEMENTARY MATERIAL

Mathematical proofs and additional material (DOI: [10.1214/23-AOAS1802SUPPA](https://doi.org/10.1214/23-AOAS1802SUPPA); .pdf). This Supplementary Material contains mathematical proofs and additional material.

Data (DOI: [10.1214/23-AOAS1802SUPPB](https://doi.org/10.1214/23-AOAS1802SUPPB); .zip). This Supplementary Material contains the data used in the paper.

REFERENCES

- BELL, D. R., LEDOIT, O. and WOLF, M. (2024). Supplement to “A novel estimator of Earth's curvature (Allowing for inference as well).” <https://doi.org/10.1214/23-AOAS1802SUPPA>, <https://doi.org/10.1214/23-AOAS1802SUPPB>
- DAVISON, A. C. and HINKLEY, D. V. (1997). *Bootstrap Methods and Their Application*. Cambridge Series in Statistical and Probabilistic Mathematics 1. Cambridge Univ. Press, Cambridge. MR1478673 <https://doi.org/10.1017/CBO9780511802843>
- GREENE, W. H. (2008). *Econometric Analysis*, sixth ed. Pearson, Upper Saddle River, NJ.
- KUHN, T. S. (1962). *The Structure of Scientific Revolutions*. Univ. Chicago Press, Chicago, IL.
- KUZII, O. and ROVENCHAK, A. (2019). What the gravitation of a flat Earth would look like and why thus the Earth is not actually flat. *Eur. J. Phys.* **40** 035008.
- LEDSON, A. (2022). Why Is Your Flight Slower Today Than Ever Before? Forbes, (published on 08-December-2022). <https://www.forbes.com/sites/alexledsom/>.
- POPPER, K. R. (1959). *The Logic of Scientific Discovery*. Hutchinson, London. MR0107593
- ROWBOTHAM, S. B. (1881). *Zetetic Astronomy: Earth Not a Globe*, third ed.
- SNYDER, P. J. (1987). *Map Projections – A Working Manual*. U.S. Geological Survey #1395.